Catalysis Letters
https://doi.org/10.1007/s10562-018-2368-6

Efficient Synthesis of Branched Polyamine Based Thermally Stable Heterogeneous Catalyst for Knoevenagel Condensation at Room Temperature

Haribandhu Chaudhuri[1] · **Radha Gupta**[1] · **Subhajit Dash**[1]

Received: 17 July 2017 / Accepted: 21 March 2018

Abstract
In this paper, a new convenient strategy for the synthesis of polyethylenimine functionalized Si-MCM-41 grafted on surface modified graphene oxide has been developed. The as-synthesised catalyst exerts good catalytic activity and reusability toward Knoevenagel condensation of different substituted aromatic aldehydes with malononitrile and ethyl cyanoacetate. Moreover, it shows remarkable thermal stability. The physicochemical characteristics of the catalyst as probed by FTIR, XRD, N_2 sorption isotherms, TGA, XPS, FESEM, TEM, and solid state ^{13}C NMR analyses, were discussed to get an idea about the catalytic mechanism of Knoevenagel condensation.

Graphical Abstract

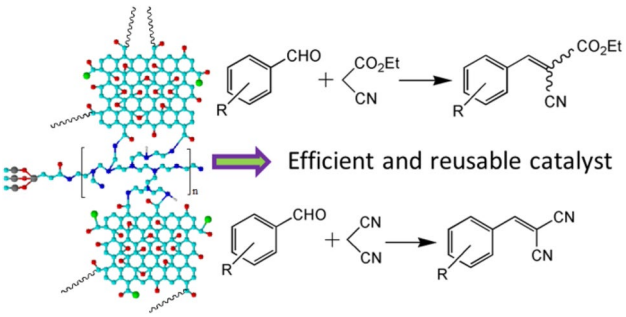

Keywords Si-MCM-41–PEI–GO catalyst · Knoevenagel condensation · Room temperature reaction · Heterogeneous catalysis

1 Introduction

Recently, graphene oxide (GO) has created tremendous awareness due to its special 2D aromatic like structure, a large surface area along with good mechanical characteristics. GO has huge number of active functional groups on its surface, which allow it to function as a catalyst [1–4] or an oxidant [5, 6]. The aromatic like scaffold and excellent surface area of GO offer a template to anchor active functional groups for catalysts [7–9]. Moreover, chemically functionalized GOs have been widely studied over the past few years and those could be executed to different organic transformations as efficient catalysts. For example, amine-modified GO

Electronic supplementary material The online version of this article (https://doi.org/10.1007/s10562-018-2368-6) contains supplementary material, which is available to authorized users.

✉ Haribandhu Chaudhuri
chaudhuri.haribandhu@gmail.com

Radha Gupta
radha.gupta1989@gmail.com

Subhajit Dash
subhajit.dash@gmail.com

[1] Organic Materials Research Laboratory, Department of Applied Chemistry, Indian Institute of Technology (Indian School of Mines), Dhanbad, Jharkhand 826004, India

Published online: 27 March 2018

could serve as base catalyst [10–12], bifunctional GO as an effective acid–base catalyst [13, 14], and sulfated GO as solid acid catalyst [15, 16]. However, the previously reported synthetic methods of GO and GO-based catalysts suffer from complex procedures, which may disturb the thermochemical stability of GO or GO-based catalyst [10, 16]. Previous workers have reported different amino functionalized materials, which were used as catalysts for Knoevenagel condensation [17–22]. Though a large number of experiments have already been done in this area, but still it is required to design more advanced inexpensive thermally stable catalyst for such type of catalytic reactions.

So, from the understanding of these view points, here we demonstrate PEI functionalized Si-MCM-41 material, which was subsequently further functionalized with surface modified GO through the formation of siloxyderivative of *n*-propylcabanoyl chloride (SPCC) intermediate (Scheme 1) [23].

In this context, Si-MCM-41 has received a significant attention due to high surface area, uniform pore radius, and good pore volume. As Si-MCM-41 is highly stable, intense efforts have been made for the synthesis of functionalized Si-MCM-41 with different active organic sites. Functionalization of Si-MCM-41 with useful organic moieties on the mesostructured silica walls creates huge scope of research [24–29]. In order to get a brief information about the synthesised Si-MCM-41–PEI–GO, various characterisations techniques were employed like Fourier transformed infrared (FTIR) spectroscopy, X-ray diffractograms (XRD), N_2 sorption measurements, thermogravimetric analysis (TGA), X-ray photoelectron spectroscopy (XPS), field emission scanning electron microscopy (FESEM), transmission electron microscopy (TEM), ^{13}C cross polarisation (^{13}C CP), magic angle spinning (MAS) NMR analyses. TGA curve shows greater thermal stability of Si-MCM-41–PEI–GO than GO possibly due to the presence of siloxane moiety of Si-MCM-41–PEI meticulously functionalized with GO. XPS analysis was carried out to get a brief insight about the elemental compositions and surface chemical state of the catalyst. FTIR, XRD, and N_2 sorption isotherms, FESEM, TEM images, and ^{13}C CP MAS NMR spectrum specified the successful formation of the catalyst. The as-synthesised catalysts offer high catalytic efficiency toward Knoevenagel condensation with short reaction time at room temperature (RT) and the used catalyst can be recycled without causing any important deformation in the catalytic activity.

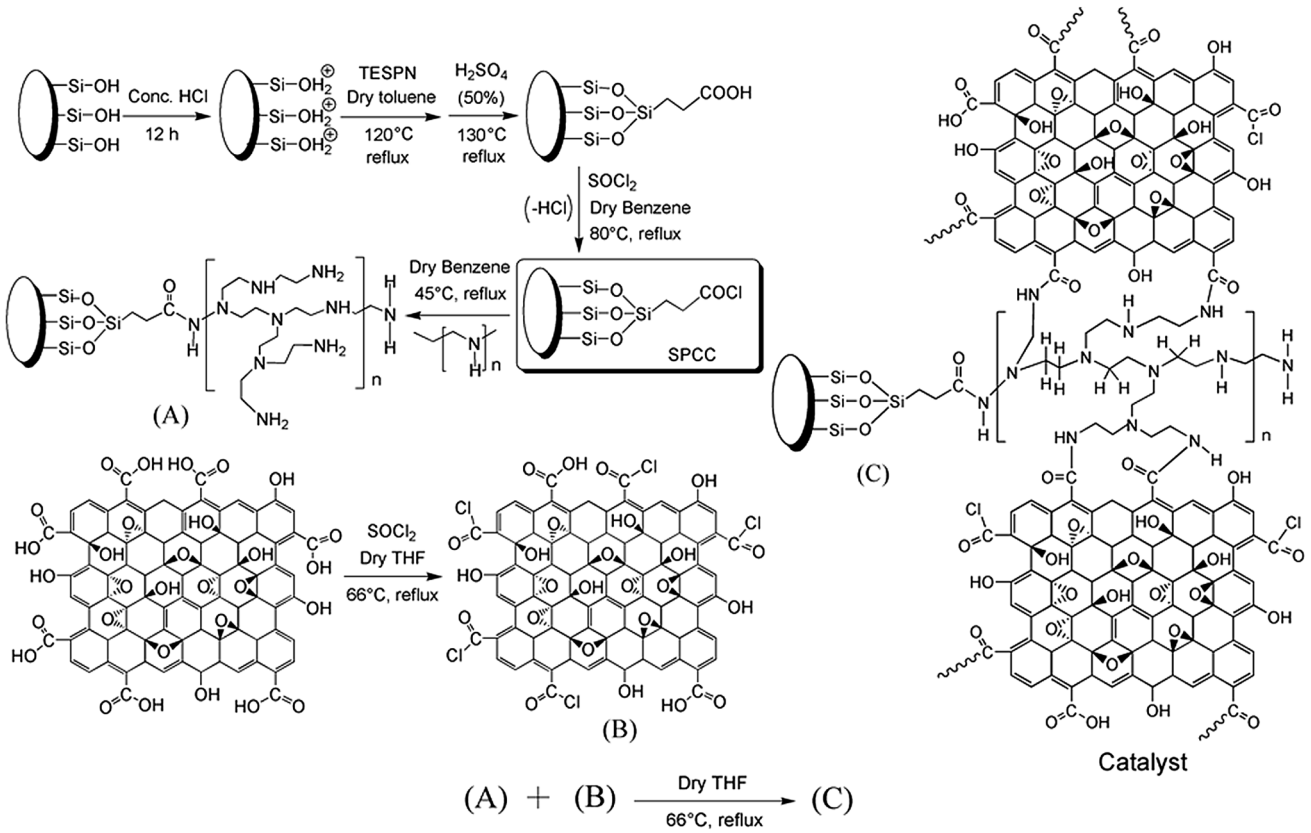

Scheme 1 Proposed scheme for the synthesis of catalyst (C)

2 Experimental Section

2.1 Materials and Reagents

Polyethyleneimine (PEI ≥ 98%), hexadecyltrimethylammonium bromide (CTAB), tetraethoxysilane (TEOS ≥ 99%), 3-(triethoxysilyl)-propionitrile (TESPN ≥ 98%), triethanolamine (TEA ≥ 99%) were procured from Sigma-Aldrich. Graphite, sulphuric acid (H_2SO_4 ~ 98%), sodium nitrate ($NaNO_3$), potassium permanganate ($KMnO_4$), hydrochloric acid (HCl ~ 37%), orthophosphoric acid (H_3PO_4 ~ 98%), silica gel (60–120 mesh), hydrogen peroxide (H_2O_2 ~ 30%), sodium thionyl chloride ($SOCl_2$), hydroxide (NaOH), and sodium sulphate (Na_2SO_4) were procured from Merck. All other solvents were purchased from Alfa Aesar. The pre-coated aluminium plates (Merck) were used for thin layer chromatography (TLC) and spots were taken under UV light. Distilled water was used throughout all the experiments.

2.2 Synthesis

Si-MCM-41 was synthesised according to the procedure described earlier [30]. In a typical process, 20.85 g of a 25 wt% CTAB solution (0.787 mmol) and 130 ml of water (0.372 mol) were taken in a round bottomed flask (RB) and stirred. After that, 0.45 g of TEA (0.21 mmol) and 23.49 ml of ethanol (0.015 mol) were combined and stirred in an oil bath at 60 °C for 1.5 h. Then, 14.9 ml of TEOS (3.253 mmol) was added dropwise to the homogeneous solution within 15 min while stirring. The solution turned white after 2.5 h. After that, the mixture was filtered, washed with distilled ethanol–water mixture and dried for 24 h under vacuum (yield ~ 98%). At last, the as-synthesised product was calcined at 520 °C for 6 h. Before functionalization, the synthesised calcined Si-MCM-41 was refluxed in concentrated HCl for 24 h. The resulting solid was extensively treated with distilled water until the material became acid free and dried at 100 °C for 24 h under vacuum.Carboxy functionalized Si-MCM-41 was prepared following the strategy reported earlier [23]. 1 g of acid treated Si-MCM-41 and TESPN (0.1 mol) in dry toluene (15 ml) were combined and stirred in RB in an oil bath at 120 °C for 24 h. Thereafter, it was consecutively treated with dry toluene and dried at 120 °C. The cyano functionalized Si-MCM-41 was refluxed with 15 ml of sulphuric acid (50%) at 110 °C for 12 h. The as-synthesised carboxy functionalized Si-MCM-41 was washed extensively with distilled water until the solid become free from acid and dried at 110 °C. Thereafter, the product was refluxed with $SOCl_2$ in presence of 15 ml of dry benzene at 80 °C for 12 h and the excess $SOCl_2$ was distilled off along with anhydrous benzene to form SPCC (Scheme 1) [23]. 1 g of SPCC was refluxed with 0.1 mol of PEI in 15 ml of dry benzene at 45 °C for 18 h. Then, the excess dry benzene was distilled off and the material was dried under vacuum.

Further, GO was prepared from graphite flakes by a modified Hammers procedure [31]. 1 g of graphite and 500 mg of $NaNO_3$ were mixed with 2.5 ml of H_3PO_4 and 25 ml of H_2SO_4 and stirred in an ice bath for 45 min. 3.2 g of $KMnO_4$ was very slowly added to the mixture to control the temperature below 5 °C. The mixture was reacted for 1.5 h in an ice bath and stirred for 1.5 h before again being stirred in an oil bath at 45 °C for 1 h. Thereafter, 50 ml of distilled water was added into the combined solution and the temperature was maintained at 100 °C for 60 min. The medium was again diluted so that the volume of the total mixture was 150 ml. 3.5 ml of H_2O_2 was added to the mixture after 1 h. Whereupon, the solution turned yellow. Finally, the as-synthesised material was centrifuged, washed with mixture of dilute acid–water repeatedly and dried at 60 °C under vacuum for 12 h. In the last step, 1 g of GO was refluxed with $SOCl_2$ in presence of 20 ml of dry THF at 66 °C for 24 h and the excess $SOCl_2$ was distilled off along with dry THF. Si-MCM-41–PEI–GO was synthesised when 1 g of Si-MCM-41–PEI and 1 g of $SOCl_2$ treated GO were combined in 30 ml of dry THF and stirred at 66 °C for 24 h and the excess dry THF was distilled off. Finally, the resulting material was washed and dried under reduced pressure.

2.3 Catalytic Experiments

For Knoevenagel condensation, finely dispersed 10 wt% Si-MCM-41–PEI–GO in 5 ml mixture of THF/benzene (1:1), prepared by sonication for 15 min, was added to a mixture of aromatic aldehyde (1 mmol) and malononitrile/ethyl cyanoacetate (1 mmol) in a 25 ml RB. The mixture was stirred for certain time and it was monitored by TLC at certain intervals. After completion, the combined solution was cooled to RT and the catalyst was removed by filtration. Thereafter, the excess mixture of THF/benzene was distilled off and the desired product was purified by flash chromatography over silica gel. The as-synthesised products were analysed by ^1H nuclear magnetic resonance (NMR) spectrometer [32, 33]. The desired data with spectra of the as-synthesised products have been presented in the Supporting Information (Figs. S2–S15).

2.4 Characterizations

FTIR analyses were performed using FTIR spectrometer (IR-Perkin Elmer, Spectrum 2000, KBr pellet technique). XRD patterns were recorded using Thermal ARL X-ray diffractometer with Cu K_α radiation source. N_2 sorption

measurements were carried out at 77 K with Nova 3200e (Quantachrome, USA). TGA (NETZSCH STA-449f3, Jupiter) curves were obtained on a thermal analyser in the temperature range 50–900 °C at a heating rate 5 °C/min in N_2 flow. XPS analysis was carried out using PHI 1600 ESCA system, Perkin Elmer. FESEM (Supra 55, Zeiss, Germany) and TEM (JEM-2100, JEOL, Japan) were carried out to determine the surface properties of catalyst. ^{13}C CP MAS NMR spectrum was obtained using ECA400 MHz instrument operated with 4 mm CD/MAS prove at RT. For catalytic reactions, the products were collected and analysed using ^{1}H NMR spectrometer operating at 400 MHz, using tetramethylsilane (TMS) as internal standard and $CDCl_3$ as solvent. δ values are reported in parts per million (ppm) and coupling constants (J) in Hertz (Hz).

3 Results and Discussion

3.1 Characterizations of the As-synthesised Catalyst

Various instrumental techniques such as FTIR, XRD, N_2 sorption isotherm, FESEM, TEM, solid state ^{13}C NMR, and XPS analysis were carried out to check the successful formation of the as-synthesised catalyst.

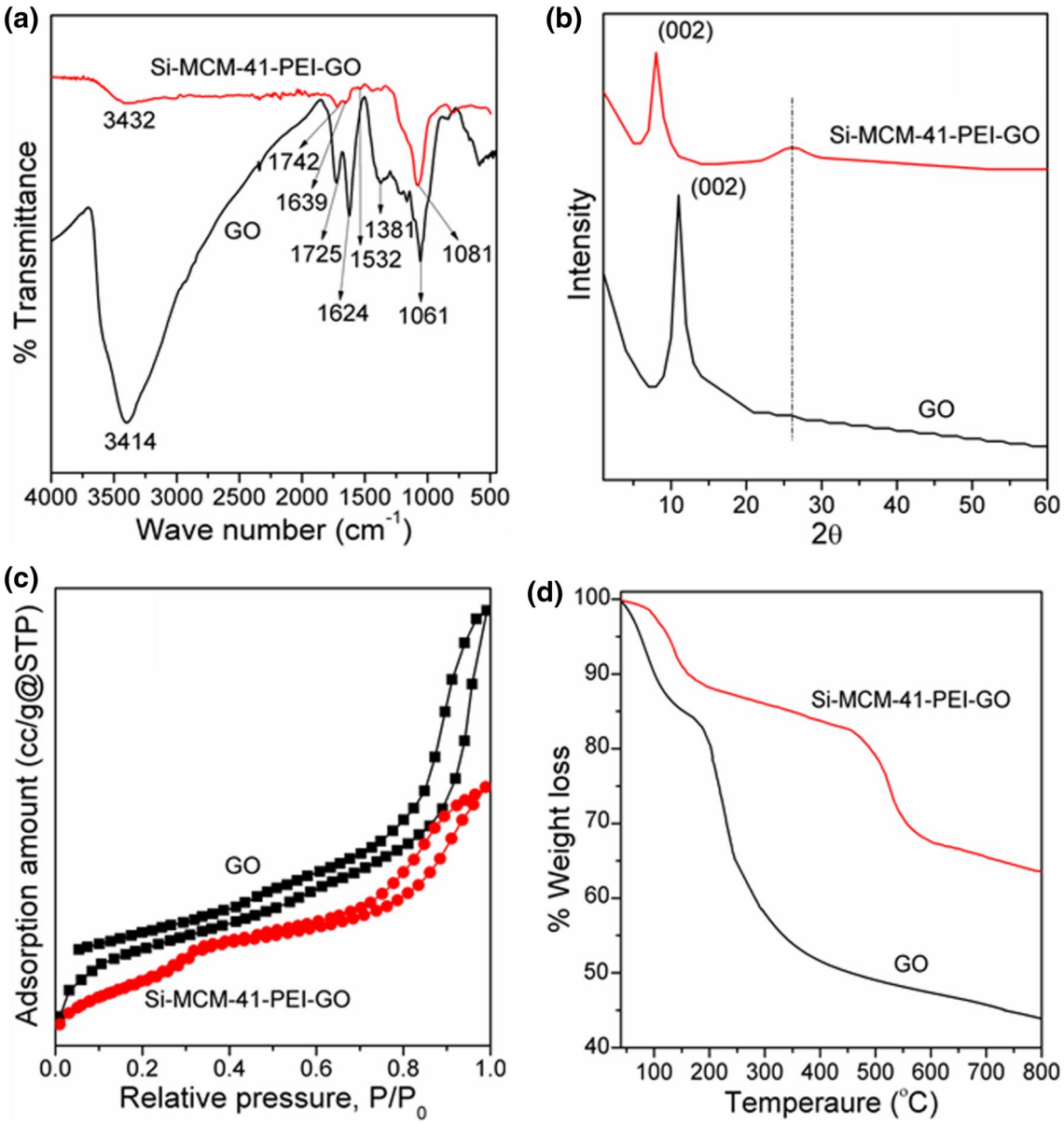

Fig. 1 FTIR spectra (**a**), XRD patterns (**b**), N_2 sorption isotherms (**c**), and TGA curves (**d**) of GO and Si-MCM-41–PEI–GO

The FTIR spectra were recorded for GO and Si-MCM-41–PEI–GO and presented in Fig. 1a.

GO shows characteristic bands at 3414 cm^{-1} (–OH stretching due to the presence of phenol and hydroxyl groups), 1725 cm^{-1} (–C=O stretching which is attributed to the presence of carbonyl and carboxylic acid groups), 1624 cm^{-1} (–OH bending of trapped H_2O molecules), 1381 cm^{-1} (due to the presence of $–CH_3$ bending vibrational modes), and 1061 cm^{-1} (–C–O stretching which is ascribed to the presence of hydroxyl groups) [34]. For Si-MCM-41–PEI–GO, –OH stretching band shifted to 3432 cm^{-1}, –C=O stretching which is attributed to the presence of carbonyl and carboxylic acid groups shifted to 1742 cm^{-1}, and –OH bending of trapped H_2O molecules moved to 1639 cm^{-1}. Si–O–Si asymmetric stretching vibrational mode has been observed at 1081 cm^{-1}. The shifting of different bonds (like –OH) indicate the formation of H-bonding between different groups in Si-MCM-41–PEI–GO, as H-bonding lowers the energies of absorption (E = hv). Beside this, the presence of symmetric $–NH_3^+$ bending vibration at 1532 cm^{-1} confirms successful functionalization of PEI on the catalyst [35, 36].

The XRD patterns (Fig. 1b) reveal a diffraction peak at 11.1°, which in accordance with the familiar (002) peak of GO [37, 38]. For Si-MCM-41–PEI–GO, (002) peak shifted at 8.2°. One possible reason might be that the structural property of the as-synthesised material plays a crucial role, for which (002) peak shifted to lower angle as compared to pure GO. Moreover, the shift of the peak in XRD may be indicative of decrease in the crystalinity of the GO on incorporation of Si-MCM-41–PEI [39]. Beside this, a broad peak centred at 26.5° is observed, which is attributed to the presence of PEI functionalised Si-MCM-41 in the synthesised catalyst.

N_2 adsorption–desorption isotherms were carried out for GO and Si-MCM-41–PEI–GO and given in Fig. 1c. A perusal of Fig. 1c reveals that GO has high surface area (389 m^2/g). For Si-MCM-41–PEI–GO, BET surface area decreases to 326 m^2/g due to the incorporation of PEI onto the surface of catalyst [35], which provides the potential of Si-MCM-41–PEI–GO for heterogeneous catalytic efficiencies.

TGA analyses were performed for GO and Si-MCM-41–PEI–GO and shown in Fig. 1d. Initially, for GO, below 100 °C, weight loss of about 5% was observed during the pretreatment of sample. All the curves indicate a decreased weight loss upto 160 °C, which is ascribed to the removal of physicochemically attached H_2O molecules of both GO and Si-MCM-41–PEI–GO. For GO, again weight loss occurred between 200 and 280 °C, due to the elimination of oxygen-containing functional groups. For Si-MCM-41–PEI–GO, weight loss occurred between 460 and 530 °C, which is attributed to the removal of PEI and detachment of Si-MCM-41 from catalyst [23]. So, it may be concluded that the greater stability of Si-MCM-41–PEI–GO over GO possibly owing to the existence of Si-MCM-41 attached to the surface modified GO.

FESEM and TEM were done for the catalyst (Fig. 2a, b).

A perusal of Fig. 2a implies a strong proof of the presence of closely attached silica particles on the GO surface. Agglomerated silica particles reveal that the presence of PEI on the surface of GO. From the inset Fig. 2a, it clearly indicates the presence of PEI attached silica particles over folded sheeted GO surface. A perusal of TEM image (Fig. 2b)

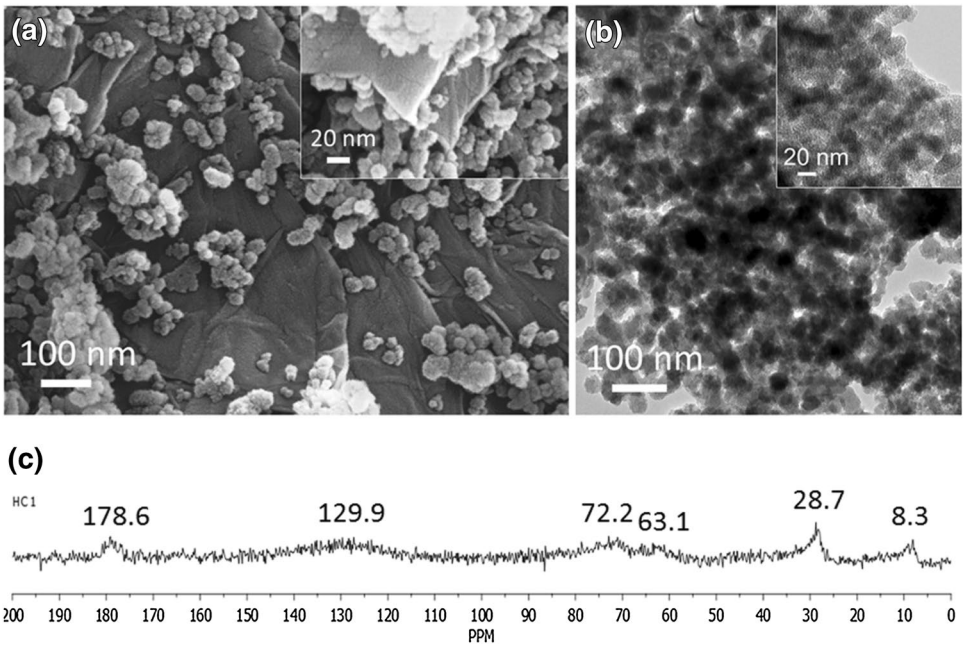

Fig. 2 FESEM (**a**), TEM (**b**), and solid state ^{13}C CP MAS NMR spectrum (**c**) of Si-MCM-41–PEI–GO, respectively

indicates that agglomeration was also observed for PEI functionalized Si-MCM-41 grafted on surface modified GO. Moreover, inset image (Fig. 2b) of Si-MCM-41–PEI–GO displays rough, agglomerated surface. This feature may have potential advantages in catalytic reactions, because reactants can easily access the active sites on the both sides of the catalyst. Thus, it may be assumed that the systematically connected mesoporosity was maintained and the successful formation of catalyst occurred.

The successful functionalisation of surface modified GO by Si-MCM-41–PEI was confirmed by solid state ^{13}C CP MAS NMR spectroscopic study. A perusal of Fig. 2c reveals the presence of peaks at 8.3 and 28.7 ppm which implies the existence of aliphatic carbon chain of PEI onto the catalyst [40]. The presence of C–O–C bond, C–OH bond, and graphitic sp^2 hybridized carbon atoms at 63.1, 72.2, and 129.9 ppm, respectively indicates the successful incorporation of GO into the catalyst [23, 40]. Furthermore, a strong signal at 178.6 ppm is attributed to the carbonyl carbon of urea bond.

XPS analysis was carried out for Si-MCM-41–PEI–GO and given in Fig. 3. According to the survey scan, silicon, oxygen, nitrogen, and carbon present on the surface of the catalyst (Fig. 3a). In order to examine the composition of the catalyst, deconvolution of Si(2p) XPS spectrum have been recorded. A perusal of Fig. 3b reveals that each Si(2p) peak consists of two $Si(2p_{3/2})$ and $Si(2p_{1/2})$ peaks due to the spin orbital coupling. The binding energies of $Si(2p_{3/2})$ and $Si(2p_{1/2})$ peaks were determined to be about 102.4 and 102.8 eV, which are consistent with the binding energy for formation of siloxane moieties [41]. Figure 3c shows the deconvoluted O(1s) XPS spectrum of the catalyst. Figure 3c reveals that each O(1s) peak has been deconvoluted into three parts, which appear due to the presence of –C=O(OH), –O–H, and C–O–C in the binding energy range of 530.4, 532.1, and 532.9 eV, respectively [42]. A perusal of Fig. 3d shows that each N(1s) peak consists of two parts, which appear due to the presence of N–C=O and N–H in the binding energy range of 399.1 and 400.8 eV, respectively [43]. Figure 3e indicates the deconvoluted C(1s) XPS spectrum of the catalyst. Each C(1s) peak has been deconvoluted into six parts, which appear due to the presence of C=C, C–OH, C–C, C–O–C, O–C=O, and C–N in the binding energy range of 286.4, 287.2, 287.4, 288.3, 289.9, and 290.7 eV, respectively [44]. Thus, all these observations indicate successful formation of Si-MCM-41–PEI–GO catalyst.

3.2 Catalytic Studies

The catalytic activity of Si-MCM-41–PEI–GO was examined for Knoevenagel condensation, as shown in Scheme 2.

The synthesised catalyst was assessed for its catalytic efficiency in Knoevenagel condensation between different substituted aromatic aldehyde (1 mmol) and malononitrile (1 mmol) (Scheme 2a) [45–47]. Initially, the reaction was carried out in absence of catalyst at RT. But, no product was formed after 720 min (Table S1, entry 1). Similarly, in absence of catalyst, at 70 °C, nothing was formed (Table S1, entry 2). The catalysts concentrations were varied in the range of 1–10 wt%. In presence of 1, 2, and 5 wt% of catalyst in mixture of THF and benzene (v/v) in 1:1 at RT, desired products (61% yield, 79% yield, and 87% yield, respectively) were found (Table S1, entry 3–5). Finally, the reaction in presence of 10 wt% of catalyst in mixture of THF and benzene (1:1) at RT results in full conversion of 4-nitrobenzaldehyde to 2-(4-nitrobenzylidene) malononitrile in short time (30 min), compared to the earlier (Table S1, entry 6). Therefore, in order to optimise the solvent effect, the reaction was carried out in different solvents. In H_2O, 38% of the desired product was formed (Table S2, entry 1). But, for THF, product yield increased to 89% (Table S2, entry 2). In mixture of H_2O and THF, 54% yield of the desired product was found (Table S2, entry 3). Only benzene gave 72% product yield within 300 min (Table S2, entry 4). Finally, the highest yield (100%) of desired product was found when the reaction was carried out in the mixture of THF and benzene (v/v) in 1:1 at RT within 30 min (Table S2, entry 5). Moreover, reactions were also carried out in CH_3CN (Table S2, entry 6), CH_2Cl_2 (Table 2, entry 7), MeOH (Table S2, entry 8), ethyl acetate (Table S2, entry 9), and toluene (Table S2, entry 10). But, results were very poor for all those cases. Again, the reaction scope was expanded to different substituted aromatic aldehydes with malononitrile under optimised conditions. The results obtained, are presented in Table 1.

The desired products obtained were characterised by ^1H NMR. Aromatic aldehydes containing electron withdrawing groups were more reactive, with complete conversion being achieved (Table 1, entries 1–4). High yields of the desired products were also observed for the aldehydes bearing electron donating groups (Table 1, entries 5–7). The conversion rates were decreased for the aldehydes bearing electron donating groups, compared to the aldehydes containing electron withdrawing groups.

A perusal of Scheme 2b reveals that Si-MCM-41–PEI–GO was further assessed for its catalytic efficacy in Knoevenagel condensation between various substituted aromatic aldehyde (1 mmol) and ethyl cyanoacetate (1 mmol) [45–47]. Similarly, the reaction was performed in absence of Si-MCM-41–PEI–GO at RT and at 80 °C, nothing was found after 960 min (Table S3, entry 1–2). In presence of 1, 2, and 5 wt% of catalyst in mixture of THF and benzene (v/v) in 1:1 at RT, desired products (59% yield, 75% yield, and 86% yield, respectively) were found (Table S3, entry 3–5). Finally, in presence of 10 wt % of catalyst in mixture of THF and benzene (1:1) at RT, 99% yield of the desired product was formed in short

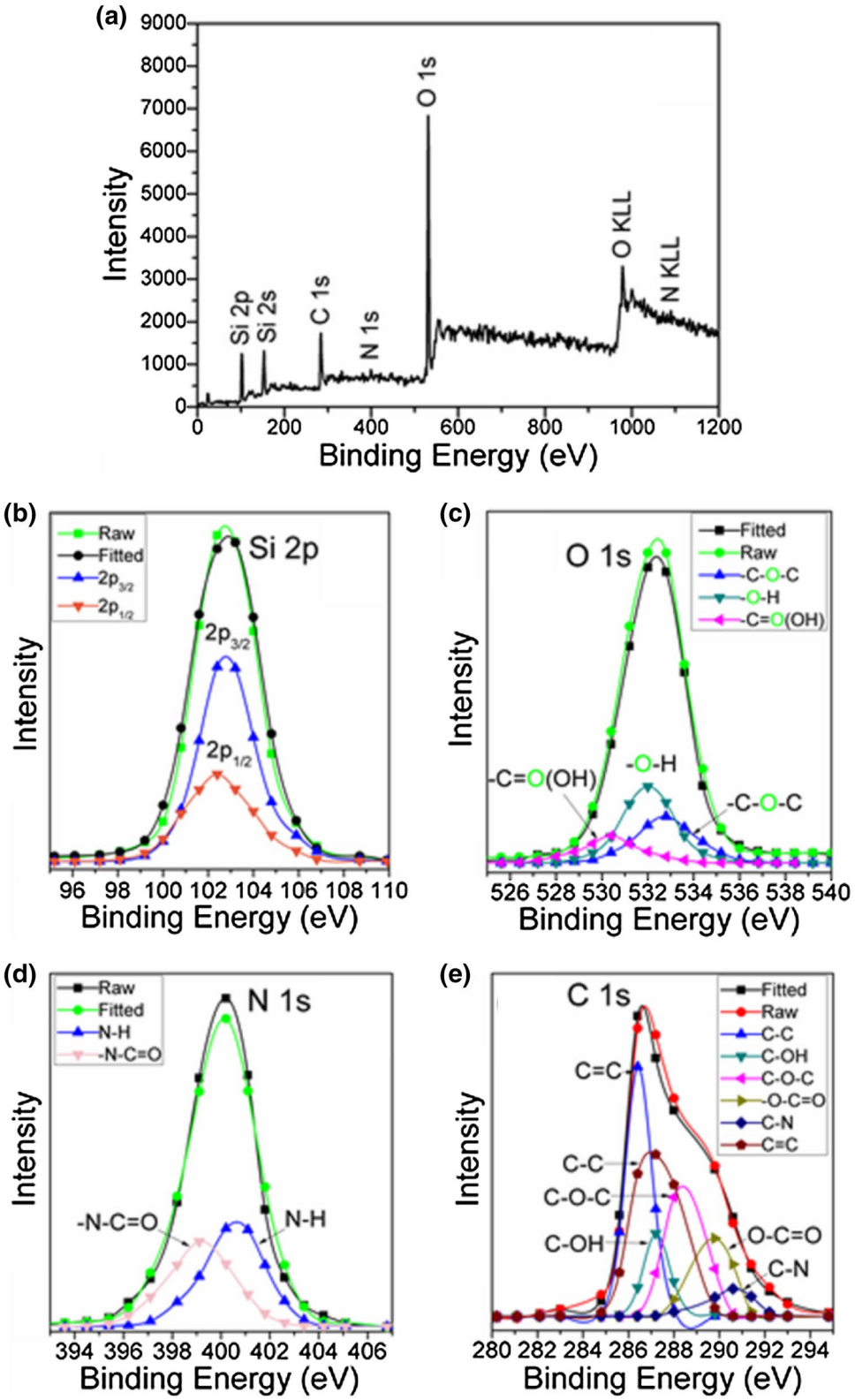

Fig. 3 Wide-scan XPS spectrum of Si-MCM-41–PEI–GO (**a**). Deconvolution of Si(2p) XPS spectrum (**b**), O(1s) XPS spectrum (**c**), N(1s) XPS spectrum (**d**), and C(1s) XPS spectrum (**e**) of Si-MCM-41–PEI–GO, respectively

reaction time (45 min), which was quite higher than earlier results (Table S3, entry 6). Thereafter, in order to standardise the effect of solvent, the reaction was performed in different solvents. In H_2O and benzene, 44 and 69% of the desired products werefound (Table S4, entry 1–2). But, in THF, product yield increased to 86% within 180 min, which was quite higher than earlier (Table S4, entry 3). In mixture of THF and benzene (v/v) in 1:1, highest

Scheme 2 Room temperature Knoevenagel condensation between substituted aldehydes and malononitrile (**a**), ethyl cyanoacetate (**b**) catalysed by Si-MCM-41–PEI–GO

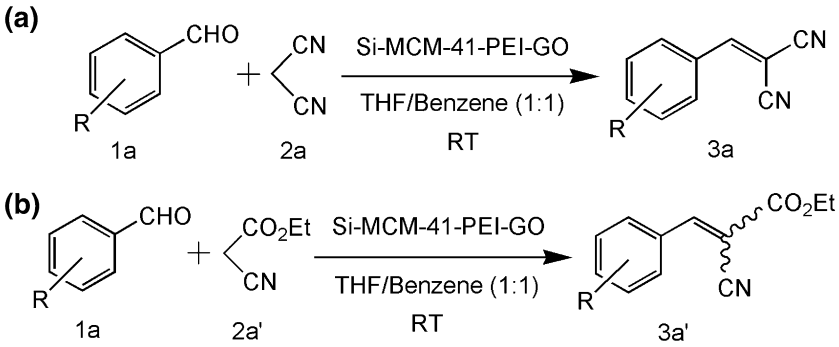

Table 1 Knoevenagel condensation of substituted aromatic aldehydes with malononitrile using Si-MCM-41–PEI–GO under the optimised reaction conditions

Entry	Aldehyde	Product[a]	Time (min)	Yield (%)[b]
1	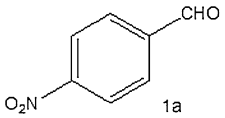	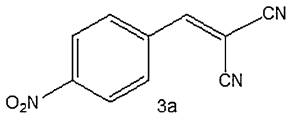	30	100
2	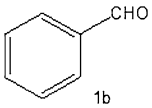	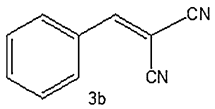	30	100
3	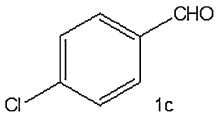	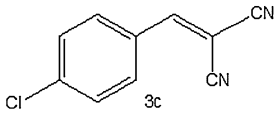	30	100
4	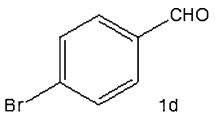	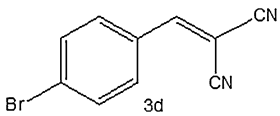	30	100
5	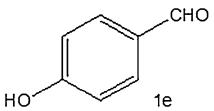	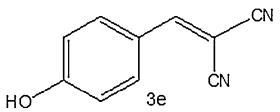	30	98
6	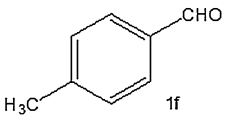	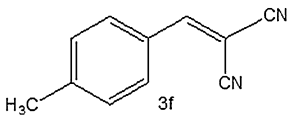	30	96
7	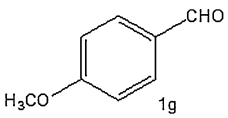	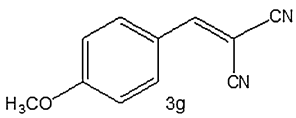	30	97

[a]Purity checked by TLC and ^{1}H NMR

[b]Isolated yield

yield (99%) of desired product was formed within 45 min (Table S4, entry 4). Fifty eight percentage of desired product was found when the reaction was carried out in the mixture of H_2O and THF (Table S4, entry 5). Moreover, reactions were also performed in toluene (Table S4, entry 6), MeOH (Table S4, entry 7), CH_2Cl_2 (Table S4, entry 8), ethyl acetate (Table S4, entry 9), and CH_3CN (Table S4, entry 10). But, results were found very low for all those cases. Again, the reaction scope was extended to various substituted aromatic aldehydes with ethyl cyanoacetate under standardised conditions and the results obtained, demonstrated in Table 2.

All the desired products (E and Z; and E/Z ratios) found were confirmed by ^{1}H NMR. High yields of the desired products were also observed for the all substituted aldehydes (Table 2). But, the conversion rates were greater for the aldehydes bearing electron withdrawing groups, compared to the aldehydes containing electron donating groups. This is due

Table 2 Knoevenagel condensation of substituted aromatic aldehydes with ethyl cyanoacetate using Si-MCM-41–PEI–GO under the optimised reaction conditions

Entry	Aldehyde	Product[a]	Time (min)	Yield (%)[b]
1	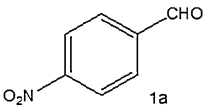 1a	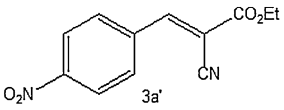 3a'	45	99 (100/0)[c]
2	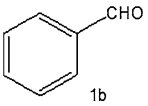 1b	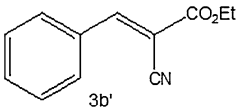 3b'	45	98 (100/0)[c]
3	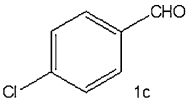 1c	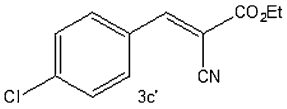 3c'	45	98 (100/0)[c]
4	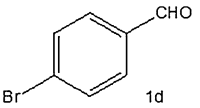 1d	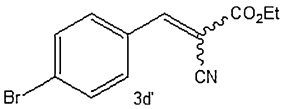 3d'	45	98 (93/7)[c]
5	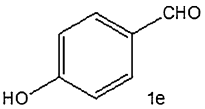 1e	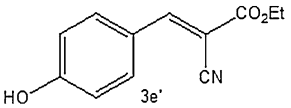 3e'	45	95 (100/0)[c]
6	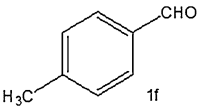 1f	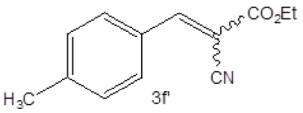 3f'	60	93 (91/09)[c]
7	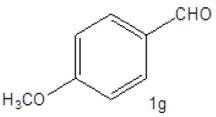 1g	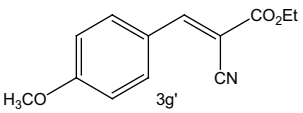 3g'	60	94 (100/0)[c]

[a]Purity checked by TLC and ^{1}H NMR

[b]Isolated yield

[c]E/Z ratio, determined by ^{1}H NMR

to the fact that the possibility of attack of the carbanion (generated from active methylene group) on the carbonyl carbon is more in case of electron withdrawing groups, compared to that of electron donating groups (Fig. 4).

Thus, it may be concluded that malononitrile shows slightly higher conversion of different substituted aromatic aldehydes, compared to ethyl cyanoacetate.

In this work, a combination of benzene and THF afforded excellent conversions for the reaction within a short reaction time (Tables S2 and S4). The reaction carried out in THF, a relatively polar solvent, also gave high yield (4-nitrobenzaldehyde with malononitrile, 89% and 4-nitrobenzaldehyde with ethyl cyanoacetate, 86%) desired product within 120 and 180 min, respectively. But, it was previously proposed that the rate of the Knoevenagel reaction using silica-based catalysts was influenced by the partitioning of the reactants (polar) between the catalyst pores and/or surface (polar) and the bulk reaction media [48, 49]. The similar trend in the effect of solvent polarity (i.e. highly polar solvents are disadvantageous) observed for Si-MCM-41–PEI–GO catalyst in this study could be rationalized based on the same factors. Beside this, GO is proficiently dispersed in THF. So, we used 1:1 THF and Benzene mixture ratio to get the best result.

3.2.1 Regeneration of Catalyst

To determine the recyclability of Si-MCM-41–PEI–GO, it was filtered and washed with dichloromethane after completion of each reaction. It has been noted that the catalyst was found to be recycled upto five consecutive cycles without affecting catalytic efficiency (Fig. S1). The catalytic efficiency of Si-MCM-41PEI–GO was quite appreciable, which in turn confirm its recyclability.

3.2.2 Plausible Catalytic Mechanism

We propose that Knoevenagel condensation is effected by catalysis of unreacted carboxyl group and a large amount of amino groups present in the catalyst. Thus, a plausible catalytic mechanism is shown in Fig. 4. Catalyst reacts with aromatic aldehyde through amino group and carboxyl group,

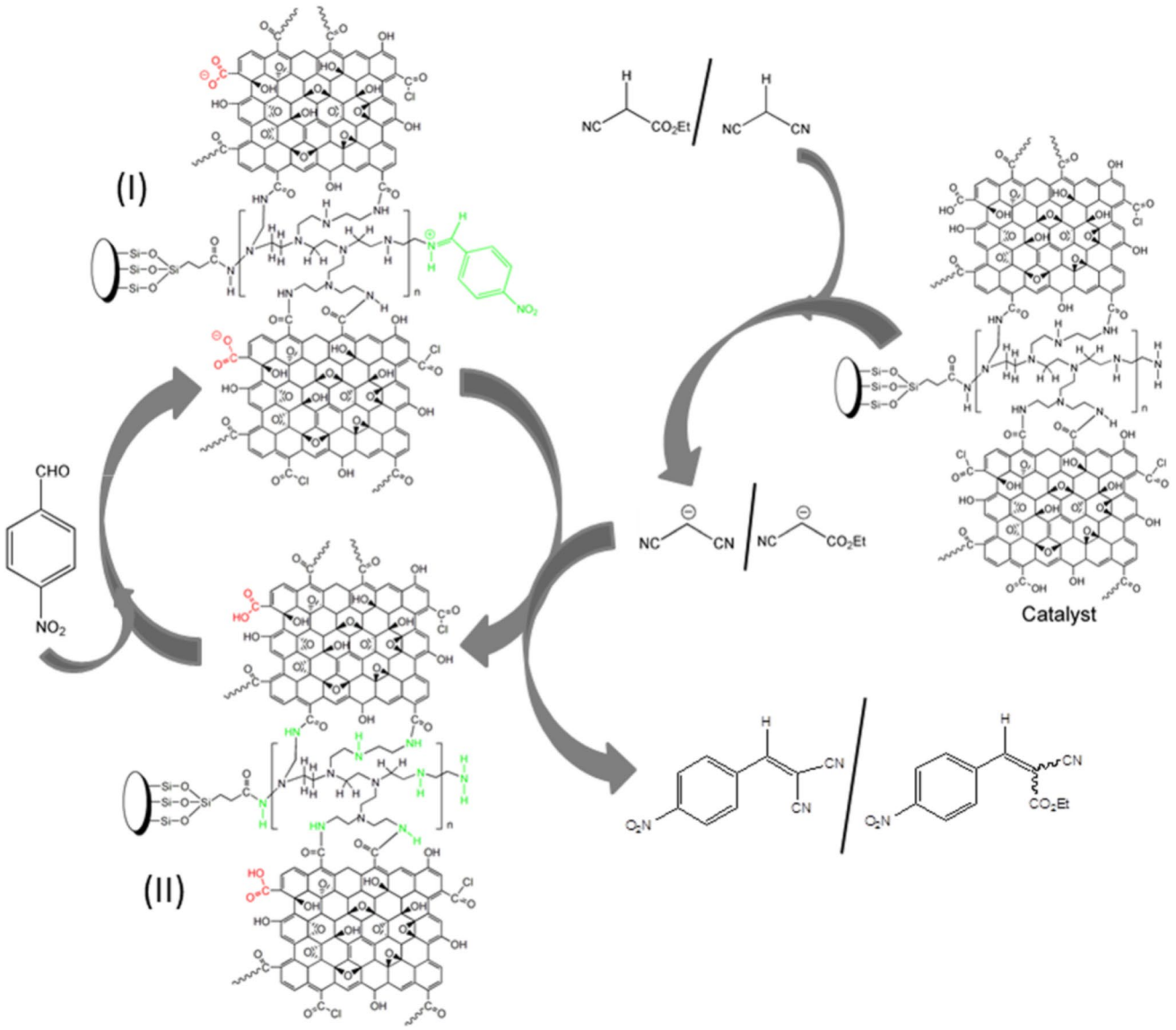

Fig. 4 Possible reaction mechanism of Knoevenagel condensation catalysed by Si-MCM-41–PEI–GO (considering 4-nitrobenzaldehyde)

resulting in an imine intermediate (I). Amino group of catalyst can act as $-H^+$ scavenger to form ethyl cyanoacetate or malononitrile anion, which plays the role of nucleophile. Thereafter, it attacks the imine intermediate (I) and in successive steps generate desired products [17–22].

4 Conclusions

To sum up, we have successfully synthesised PEI functionalised Si-MCM-41 grafted on surface modified GO, which provides a simple way to get inexpensive heterogeneous catalyst. The synthesised material has an excellent thermal stability along with high surface area. The obtained catalyst results in excellent catalytic activity toward Knoevenagel condensation with high yielded desired products. Moreover, Si-MCM-41–PEI–GO can be recovered and reused in the consecutive runs without loss of reactivity. In a broader viewpoint, these results established the use of Si-MCM-41–PEI–GO in synthetic chemistry, and it could create new catalytic applications especially in the development of amine based GO–silica hybrid materials with desired characteristics in future.

Acknowledgements HC would like to thank SAIF, Punjab University, India for NMR facility.

Compliance with Ethical Standards

Conflict of interest The authors declare no competing financial interest.

References

1. Dhakshinamoorthy A, Alvaro M, Concepción P, Fornés V, Garcia H (2012) Chem Commun 48:5443–5445
2. Dhakshinamoorthy A, Alvaro M, Puche M, Fornés V, Garcia H (2012) ChemCatChem 4:2026–2030
3. Kumar AV, Rao KR (2011) Tetrahedron Lett 52:5188–5191
4. Verma S, Mungse HP, Kumar N, Choudhary S, Jain SL, Sain B, Khatri OP (2011) Chem Commun 47:12673–12675
5. Mirza-Aghayan M, Boukherroub R, Nemati M, Rahimifard M (2012) Tetrahedron Lett 53:2473–2475
6. Dreyer DR, Jia HP, Bielawski CW (2010) Angew Chem Int Ed 49:6813–6816
7. Scheuermann GM, Rumi L, Steurer P, Bannwarth W, Mülhaupt R (2009) J Am Chem Soc 131:8262–8270
8. Chaudhuri H, Dash S, Gupta R, Pathak DD, Sarkar A (2017) ChemistrySelect 2:1835–1842
9. Zhang N, Qiu H, Wang W, Li Y, Wang X, Gao J (2011) J Mater Chem 21:11080–11083
10. Zhang Y, Chen C, Wu G, Guan N, Li L, Zhang J (2014) Chem Commun 50:4305–4308
11. Wu T, Wang X, Qiu H, Gao J, Wang W, Liu Y (2012) J Mater Chem 22:4772–4779
12. Rodrigo E, Alcubilla BG, Sainz R, Fierro JLG, Ferrittob R, Cid MB (2014) Chem Commun 50:6270–6273
13. Zhang W, Zhao Q, Liu T, Gao Y, Li Y, Zhang G, Zhang F, Fan X (2014) Ind Eng Chem Res 53:1437–1441
14. Zhang F, Jiang H, Li X, Wu X, Li H (2014) ACS Catal 4:394–401
15. Wei Z, Yang Y, Hou Y, Liu Y, He X, Deng S (2014) ChemCatChem 6:2354–2363
16. Ji J, Zhang G, Chen H, Wang S, Zhang G, Zhang F, Fan X (2011) Chem Sci 2:484–487
17. Wang X, Lin KSK, Chan JCC, Cheng S (2005) J Phys Chem B 109:1763–1769
18. Phan NTS, Jones CW (2006) J Mol Catal A 253:123–131
19. Wu T, Wang X, Qiu H, Gao J, Wang W, Liu Y (2012) J Mater Chem 22:4772–4779
20. Islam SM, Roy AS, Dey RC, Paul S (2014) J Mol Catal A 394:66–73
21. Yang A, Li J, Zhang C, Zhang W, Ma N (2015) Appl Surf Sci 346:43–450
22. Stein A, Melde BJ, Schroden RC (2000) Adv Mater 12:1403–1419
23. Chaudhuri H, Dash S, Sarkar A (2016) Ind Eng Chem Res 55:10084–10094
24. Olkhovyk O, Jaroniec M (2005) J Am Chem Soc 127:60–61
25. Karin M, Thomas B (1998) Chem Mater 10:2950–2963
26. Zhuang X, Wan Y, Feng C, Shen Y, Zhao D (2009) Chem Mater 21:706–716
27. Zhang Y, Qiao ZA, Li Y, Liu Y, Huo Q (2011) J Mater Chem 21:17283–17289
28. Shieh FK, Hsiao CT, Wu JW, Sue YC, Bao YL, Liu YH, Wan L, Hsu MH, Deka JR, Kao HM (2013) J Hazard Mater 260:1083–1091
29. Qiao Z, Zhang L, Guo M, Liu Y, Huo Q (2009) Chem Mater 21:3823–3829
30. Ho KY, McKay G, Yeung KL (2003) Langmuir 19:3019–3024
31. Hummers WS, Offeman RE (1958) J Am Chem Soc 80:1339
32. Mitra AK, De A, Karchaudhuri N (1999) Synth Commun 29:2731–2739
33. Keithellakpam S, Moirangthem N, Laitonjam WS (2015) Ind J Chem 54B:1157–1161
34. Kumari S, Shekhar A, Mungse HP, Khatri OP, Pathak DD (2014) RSC Adv 4:41690–41695
35. Chaudhuri H, Dash S, Sarkar A (2016) New J Chem 40:3622–3634
36. Nayab S, Farrukh A, Oluz Z, Tuncel E, Tarique SR, Rahman H, Kirchhoff K, Duran H, Yameen B (2014) ACS Appl Mater Intrefaces 6:4408–4417
37. Kou L, Gao C (2011) Nanoscale 3:519–528
38. Stankovich S, Dikin DA, Piner RD, Kohlhaas KA, Kleinhammes A, Jia Y, Wu Y, Nguyen ST, Ruoff RS (2007) Carbon 45:1558–1565
39. Kumari S, Shekhar A, Pathak DD (2016) RSC Adv 6:15340–15344
40. Ribeiro SM, Serra AC, Gonsalves ADAR (2011) Appl Catal A 399:126–133
41. Wagner CD, Hilery DE, Kinisky TG, Six HA, Perez-Robles JF, Zamorano-Ulloa R, Gonzalez-Hernandez J (2004) J Phys Chem Solids 65:1045–1052
42. Chaudhuri H, Dash S, Sarkar A (2016) RSC Adv 6:99444–99454
43. Zhou X, Pan Y, Xu J, Wang A, Wu S, Shen J (2015) RSC Adv 5:105855–105861
44. Yu J, Xu C, Tian Z, Lin Y, Shi Z (2016) New J Chem 40:2083–2088
45. Liu Q, Ai H, Li Z (2011) Ultrason Sonochem 18:477–479
46. Liu Q, Ai HM (2012) Synth Commun 42:3004–3010
47. Liu Q, Ai HM, Feng S (2012) Synth Commun 42:122–127
48. Macquarrie DJ, Clark JH, Lambert A, Mdoe JEG, Priest A (1997) React Funct Polym 35:153–158
49. Macquarrie DJ, Jackson DB (1997) Chem Commun 18:1781–1782